Design and Development of a Wireless Functional Electrical Stimulation and m-Health Application for Foot Drop Using an IoT-Based Architecture

Jirawat Jitprasutwit[1], Anan Banharnsakun[2], Kathawach Satianpakiranakorn[3] and Kanjana Eiamsaard[4*]

[1,2,3,4]Department of Computer Engineering, Faculty of Engineering at Sriracha, Kasetsart University Sriracha Campus, Thailand

Email : jirawat@eng.src.ku.ac.th, ananb@ieee.org, kathawach@eng.src.ku.ac.th, kanjana@eng.src.ku.ac.th*

Received: May 30,2025 / Revised: September 29, 2025 / Accepted: October 20, 2025

***Abstract*—To enhance accessibility in foot drop rehabilitation, this study presents the design and development of a wireless functional electrical stimulation system integrated with a mobile health (m-Health) application and an ESP32-based IoT (Internet of Things) platform. The system comprises a stimulation node and a sensor node that communicate via Bluetooth Low Energy (BLE) for heel-strike-triggered stimulation. The stimulation node delivers symmetrical biphasic pulses to the peroneal nerve with adjustable parameters. A cloud-based backend using MQTT supports real-time logging and device management, while the m-Health application enables mode selection, parameter tuning, and usage tracking. Key hardware includes a 70V boost converter, programmable current limiter, and H-bridge pulse generator. Evaluations show reliable pulse output (400.3 µs width, 2.1 µs rise/fall), low BLE latency (6.16 ms), and accurate analog-to-digital converter readings. Results confirm the system's feasibility as a compact, portable solution for home-based rehabilitation, addressing limitations of traditional wired systems.**

***Index Terms*— Functional Electrical Stimulation (FES), Foot Drop, Home-based Rehabilitation, Wireless Sensor, Biphasic Pulse Generation, IoT, Embedded System, m-Health Application**

I. Introduction

Stroke remains one of the leading causes of long-term disability worldwide, especially among the elderly and individuals with underlying conditions such as diabetes and hypertension. According to the World Health Organization (WHO) in 2022, nearly 15 million people suffer a stroke each year, with more than 5 million experiencing significant motor impairments that affect their ability to perform daily activities such as grasping, standing, and walking [1], [2].

One of the most common post-stroke complications is foot drop, a condition in which patients are unable to lift the front part of their foot due to muscle weakness or paralysis. This impairment causes the toes to drag while walking, increasing the risk of falling and significantly impacting mobility and independence [2]. To handle foot drop, patients often rely on Ankle-Foot Orthoses (AFOs), which help position the foot during gait. However, prolonged use of AFOs may lead to muscle atrophy from disuse [3]. Functional Electrical Stimulation (FES) offers an alternative by applying timed electrical impulses to the affected muscles or nerves, typically triggered by sensors placed on the heel while walking. In addition to improving gait by enabling dorsiflexion during the swing phase, FES has been shown to prevent muscle atrophy and support motor relearning through enhanced neuroplasticity [4]-[6]. Recent clinical studies have demonstrated that FES can improve walking speed, endurance, and balance in stroke survivors with foot drop, contributing to long-term improvements in mobility and functional independence [7]-[9]. Other treatments include physical therapy, muscle strengthening exercises, and surgical interventions when necessary [10].

A prior study developed and distributed a functional electrical stimulator for foot drop patients through regional hospitals in Thailand [11]. Subsequent clinical research conducted using that system demonstrated its effectiveness in improving walking speed and mobility among patients [4], [5]. Building upon the clinically validated Dearndee FES system previously distributed in regional hospitals, this study introduces a new wireless platform aimed at improving mobility and user engagement through modern IoT and mobile health technologies.

In response to these challenges, this study presents the design and development of a compact, wireless

FES system intended to assist individuals with foot drop. The proposed system comprises a stimulator node that delivers electrical pulses to the peroneal nerve area, a sensor node that detects heel pressure during walking, and a mobile application for device control and monitoring. Communication between nodes is achieved through Bluetooth Low Energy (BLE), supporting real-time, cable-free interaction among system components.

The design emphasizes technical aspects through the integration of custom-designed hardware, firmware, and wireless communication protocols to ensure low-latency performance and accurate electrical stimulation. A microcontroller is utilized to generate precise stimulation waveforms and manage synchronized communication between the sensor and stimulator nodes. In addition, the Mobile Health (m-Health) application is developed not only as a user interface but also as a platform for data logging and remote configuration. It is designed based on the Mobile Health (m-Health)Technology Acceptance Model (MoHTAM) [12], and follows guideline themes for Mobile Health system usability and accessibility as proposed in [13], ensuring that it meets standards for practical deployment in real-world scenarios.

While this paper does not involve human trials to avoid ethical concerns, this study demonstrates the system's technical feasibility and performance through electrical measurements, establishing a foundation for future home-based rehabilitation applications and clinical validation.

II. Background and Knowledge

This section outlines the foundational principles and design considerations underlying the proposed system, encompassing the FES methodology, electrical signal parameters, microcontroller platform, and mobile health application integration.

A. Functional Electrical Stimulation

FES applies electrical pulses to peripheral nerves to induce muscle contractions for restoring specific motor functions. For foot drop, FES stimulates the common peroneal nerve to activate dorsiflexion during gait, aiding mobility and preventing muscle atrophy. This study focuses on its application in gait rehabilitation for stroke patients [14], [15].

B. Electrical Signal Parameters

The effectiveness of FES depends heavily on how the electrical signals are configured. In this study, stimulation signals are designed based on three key parameters: Waveform, frequency, and pulse characteristics, including durtion and Intensity.

- Waveform

A symmetrical biphasic waveform was used to reduce skin irritation and prevent charge buildup, providing balanced current flow and improved comfort. Its symmetry supports precise motor unit activation, crucial for functions like foot dorsiflexion. Controlled waveform parameters also enhance stimulation selectivity and reduce fatigue [16], [17] holding a toothbrush, standing, and walking. The technology was developed in the sixties, during which initial clinical use started, emphasizing its potential as an assistive device. Since then, functional electrical stimulation has evolved into an important therapeutic intervention that clinicians can use to help individuals who have had a stroke or a spinal cord injury regain their ability to stand, walk, reach, and grasp. With an expected growth in the aging population, it is likely that this technology will undergo important changes to increase its efficacy as well as its widespread adoption. We present here a series of functional electrical stimulation systems to illustrate the fundamentals of the technology and its applications. Most of the concepts continue to be in use today by modern day devices. A brief description of the potential future of the technology is presented, including its integration with brain–computer interfaces and wearable (garment. Fig. 1 illustrates the waveform structure implemented in the system.

- Frequency

The stimulation frequency directly influences the nature of muscle contraction. Frequencies in the range of 40 Hz to 100 Hz were considered optimal for producing tetanic muscle contractions, which are essential for effective foot lifting [11], [17]. Frequencies outside the optimal range can cause either fatigue or weak contractions, so the system allows real-time frequency adjustment based on patient response.

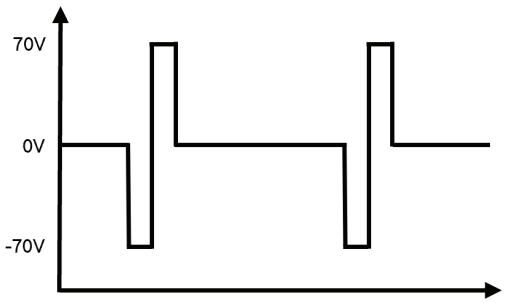

Fig. 1. A symmetrical biphasic waveform

- Pulse Duration and Intensity

Pulse duration and intensity are key to effective muscle activation, but individual differences require adjustable settings. This system allows tuning of pulse width and voltage, typically using 100-1000 µs pulses, 10-100 Hz frequency, and 60-70 V output [11], [17]. Parameters were chosen through initial testing to balance effective contraction with user comfort and minimal fatigue [18]. Stimulation parameters are adjustable in real time to match individual responses and reduce overstimulation risk.

C. Microcontroller and BLE Communication

The system employs the ESP32 microcontroller, which features a dual-core Xtensa LX6 processor operating at up to 240 MHz, with integrated Wi-Fi and BLE capabilities. ESP32 was selected over platforms such as nRF52, STM32, or Arduino due to its unique combination of built-in wireless connectivity, low cost, dual-core architecture, and native support for real-time task scheduling via Free RTOS. This architecture enables the system to handle concurrent operations efficiently, with BLE controller tasks assigned a high priority to meet real-time requirements [19]. BLE enables low-latency, energy-efficient communication between components, which is crucial for synchronized stimulation and sensing [20]. Its implementation using ESP32 modules is detailed in the hardware design section.

III. Literature Review

Functional electrical stimulation has long been established as a rehabilitative solution for foot drop, particularly among stroke survivors and individuals with neurological disorders. Over the past decade, significant advancements in embedded systems, sensor technologies, and wireless communication have influenced the design of both academic and commercial FES systems, aiming to improve usability, adaptability, and accessibility.

Early academic implementations of FES focused on basic stimulation functionality. Bhattacharya and Manjunatha reviewed microcontroller-based FES systems with capabilities for precise current modulation but noted that such systems often lacked real-time personalization and mobile connectivity, which limited their practical usability in home rehabilitation settings [21]. Jitprasutwit *et al*. presented a culturally adapted, cost-sensitive FES system for Thai users, utilizing wired stimulation without advanced feedback or wireless features [11]. Melo *et al*. advanced FES control by incorporating continuous motion feedback from the foot, allowing real-time modulation of stimulation patterns during gait [22]. The emergence of wireless technology, particularly BLE, led to portable and user-friendly system designs. Watanabe et al. developed a portable FES rehabilitation prototype featuring inertial sensors for gait event detection and Bluetooth communication with a tablet, enabling stimulation based on real-time sensor data [23]. Aqueveque *et al*. introduced a capacitive step sensor positioned under the heel, which achieved accurate real-time detection of swing-phase transitions and transmitted synchronization signals wirelessly, enhancing timing precision for stimulation delivery [24]. Additionally, York and Chakrabarty conducted a comprehensive survey highlighting the clinical effectiveness of FES in improving walking speed, quality of life, and patient preference over alternatives like AFOs, though challenges remained with system cost and sensory feedback integration [25].

In the past five years, low-cost, open-platform FES solutions have gained traction in academic research. Kipli et al. developed an Arduino Nano-based FES prototype suitable for educational or prototyping purposes, focusing on simplicity and affordability, but lacking advanced features such as mobile connectivity or AI-assisted control [26]. De Almeida et al. presented a 4-channel IoT-enabled electro stimulator using ESP32, capable of closed-loop joint angle control via inertial feedback and MQTT protocol, though it did not integrate a mobile application [27]. Gangadharan et al. introduced an intelligent system with sensor-based auto-triggering to enhance timing precision [28]. Chiriac et al. followed with a design focused on cost-effectiveness and usability in low-resource environments, though the system remained basic in function and lacked BLE or application integration [29]. Most recently, Cao et al. proposed a wearable ultrasound-FES integrated system capable of high-accuracy intention recognition using muscle thickness detection. This allowed precise real-time control of stimulation, although no mobile application or user interface for direct interaction was described [30].

In parallel, several commercial systems have been developed with higher performance but significantly higher costs. The Bioness L300 Go, for instance, integrates 3D motion sensors and mobile connectivity to optimize stimulation timing but is priced over $6,000 [31]. The WalkAide uses tilt sensors for gait detection and real-time stimulation but lacks mobile programmability [32]. Meanwhile, XFT-2001D, marketed as a semi-intelligent foot drop stimulator, features MEMS sensors and AI algorithms for adaptive output, with mobile application control, at a cost exceeding $2,199 [33].

In terms of intellectual property, patents such as US20170106189A1 present a system with multi-pad electrodes and movement sensors for adaptive stimulation control [34], while US11406821B2 outlines a compact, waterproof, stainless-steel integrated apparatus with ergonomic design features aimed at long-term usability [35].

Existing FES systems often trade off between cost and functionality. Commercial devices offer advanced features but lack flexibility, while academic prototypes are affordable yet limited in control and connectivity. This study proposes an IoT-based FES system with BLE-triggered stimulation, adjustable parameters, application control, and cloud monitoring to bridge that gap.

IV. Research Methodology

This study follows an engineering design research methodology to evaluate the feasibility of a wireless Functional Electrical Stimulation (FES) system for foot drop rehabilitation. The methodology was structured into five main stages.

A. Research Framework

The research focused on designing, prototyping, and validating a compact wireless FES system without human trials. The objective was to demonstrate technical feasibility through engineering tests of system components, communication performance, and power efficiency.

B. Hardware Methodology

The hardware was developed using a modular approach that separated the system into a stimulation node and a sensor node. The stimulation node was designed to generate programmable biphasic pulses, while the sensor node detected heel pressure and transmitted signals wirelessly through BLE. Both nodes were implemented on ESP32-based platforms due to their integrated wireless capability and suitability for real-time applications. This methodology enabled iterative prototyping and testing before full integration, while detailed hardware schematics and circuit descriptions are presented in Section V.

C. Firmware Methodology

The firmware was developed on the ESP32 platform with an interrupt-driven approach to achieve precise pulse timing and modular task organization to support real-time operation. Its main functions included pulse control, stimulation logic, BLE communication, and cloud connectivity, with implementation details described in Section V.

D. Mobile Application Methodology

The mobile application proposed in this study was constructed using the Agile development methodology. The process began with developing user stories related to rehabilitation activities. The most critical stories were then selected for development in the first iteration. After these stories were verified to be working properly, subsequent increments were developed until all user stories were completed. Finally, all functionalities were verified during the system testing process. Detailed application features and interfaces are presented in Section V.

E. Experimental Methodology

The evaluation was conducted through a structured set of experiments designed to validate system functionality. These included verification of the boost converter and current limiter circuits, assessment of waveform precision, benchmarking of ADC accuracy, measurement of BLE latency across multiple trials, and testing of battery life under continuous operation. Experiments were performed in a controlled environment using calibrated instruments to ensure accuracy. The complete setup and parameters are described in Section VI.

V. Proposed System Architecture and Design

The proposed FES system for foot drop consists of three components: A sensor node, a stimulation node, and an m-Health application. As shown in Fig. 2, the sensor node, placed near the ankle, detects foot plantar flexion and transmits real-time gait data to the stimulation node via BLE [24]. Upon receiving the trigger, the stimulation node delivers electrical stimulation to the common peroneal nerve to induce dorsiflexion and assist the user during the swing phase [4], [5], [25]. In addition to real-time stimulation control, the stimulation node collects usage data and periodically synchronizes with the cloud server, which serves as a remote repository for long-term storage and activity logging [36].

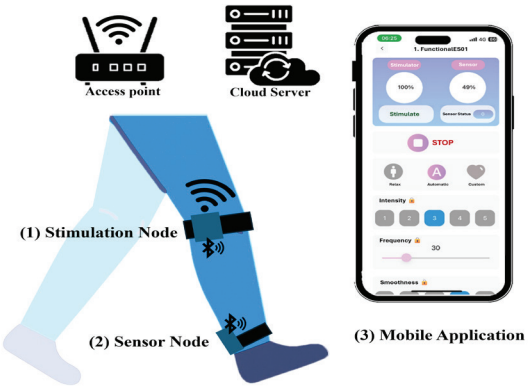

Fig. 2. System overview of the proposed FES platform for foot drop: (1) Stimulation Node for delivering electrical pulses, (2) Sensor Node for gait event detection, and (3) Mobile Application for parameter control and monitoring

The mobile application enables users or clinicians to configure stimulation parameters, monitor system performance, and visualize historical usage data. It serves as the primary interface for interacting with the system outside the stimulation hardware.

The system leverages BLE for communication between the sensor and stimulation nodes [24], while internet connectivity (via Wi-Fi or mobile hotspot) supports data exchange between the stimulation node, cloud server, and mobile application [36]. The cloud communication architecture follows IoT design principles [37], utilizing the MQTT protocol for real-time messaging with a Node-RED-based server and NoSQL database for user and session data storage [38].

When such a system is in an offline mode, the stimulation node operates using saved settings, with basic onboard adjustments.

This study focuses on system-level design across hardware, firmware, communication, and mobile interface. Initial tests evaluate latency, control response, parameter tuning, and data synchronization to support future clinical validation.

A. Hardware Design

The proposed FES system comprises two ESP32-based modules: a sensor node (M5StickC Plus) for heel-pressure detection and BLE signaling, and a stimulation node (M5Stack) for generating programmable biphasic pulses using boost, current limit, and pulse control circuits. As shown in Fig. 3, this compact design supports real-time, low-latency operation suitable for wearable FES applications.

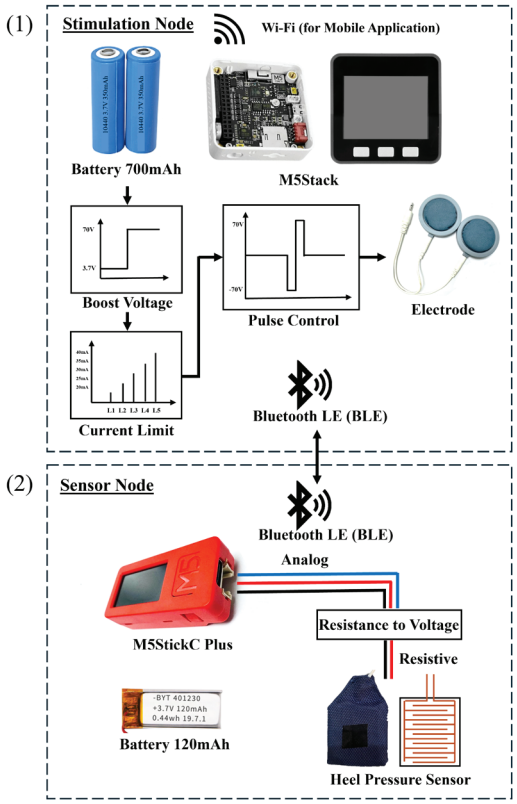

Fig. 3. Hardware architecture of the proposed FES system, consisting of (1) Stimulation Node and (2) Sensor Node

1) Stimulation Node Design

The stimulation node serves as the system's output module, delivering electrical pulses for gait rehabilitation. It is built on the M5Stack, which includes a dual-core ESP32, Wi-Fi/BLE, a 2.0-inch IPS LCD, and three user buttons [39]. This platform was chosen for its modularity and high level of integration, which allows for rapid prototyping and reduces the need for extensive peripheral circuit design [40], [41]. Although the default configuration includes a small internal battery, it was removed in this implementation to support an external 3.7 V 520 mAh lithium polymer battery, providing sufficient capacity for stimulation tasks.

The stimulation node integrates three main circuits: a boost converter (3.7 V to 70 V), a current limiter for user safety, and a pulse generator for symmetrical biphasic waveforms. These are managed by the ESP32, which handles BLE input from the sensor node and Wi-Fi communication with the cloud and mobile application. Physical switches on the M5Stack allow offline control and testing. Key specifications are shown in TABLE I, with the system structure illustrated in Fig. 3 (1).

TABLE I
TECHNICAL SPECIFICATIONS OF THE STIMULATION NODE HARDWARE

Feature	Stimulation Node	Sensor Node
Microcontroller	ESP32-D0WDQ6-V3 (240 MHz dual-core Xtensa 32-bit LX6, 520 KB SRAM)	ESP32-PICO-D4 (240 MHz dual-core Xtensa 32-bit LX6, 520 KB SRAM)
Platform	M5Stack [45]	M5Stick C Plus [46]
Flash Memory	4 MB	4 MB
Wireless Connectivity	Wi-Fi 802.11 b/g/n, Bluetooth 4.2 (BLE)	Wi-Fi 802.11 b/g/n, Bluetooth 4.2 (BLE)
Display	2.0 IPS TFT LCD, 320p×240p	1.14 IPS TFT LCD, 135p×240p
Interfaces	3x programmable buttons, USB Type-C, 26 GPIO pins, GROVE (I²C/UART)	1x programmable button, USB Type-C, 14 GPIO, GROVE (I²C/UART)
Battery	External 3.7 V Li-Po (520 mAh)	Internal 3.7 V Li-Po (120 mAh)
Dimensions (mm)	54 × 54 × 17	48.2 × 25.5 × 13.7
Weight	**45 g**	**24 g**

a) Boost Voltage Circuit

The boost circuit steps up the 3.7 V Li-Po battery to ~70 V using the ZXSC410 DC-DC controller [42], It employs an inductor (22 µH), a MOSFET (IRLML0100), a fast diode (BAS516), and a feedback divider (R1, R2) to ensure stable high-voltage output with low ripple. The regulation is based on the ZXSC410's 300 mV reference, as expressed in (1)

$$V_{out} = V_{FB}\left(1 + \frac{R1}{R2}\right) \quad (1)$$

Assuming R1 = 1 MΩ and V_{FB} = 300 mV, the required value of R2 to achieve 70 V output can be calculated using (2).

$$R2 = \left(\frac{V_{FB}R1}{V_{out} - V_{FB}}\right) = 4{,}304.16\Omega \quad (2)$$

By selecting R2 = 4.3 kΩ, the output voltage is regulated at approximately 70.07 V, which meets the system requirement. The final boost converter configuration and component placement are illustrated in Fig. 4.

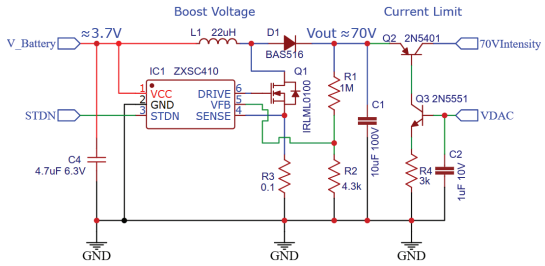

Fig. 4. Schematic of the stimulation node, showing the boost converter using ZXSC410 for 70 V output and the current limit circuit for VDAC-controlled stimulation

b) Current Limit Circuit

To ensure safe and programmable stimulation, the system incorporates a current limit circuit that regulates output current independently of voltage amplitude. A PNP transistor (Q2, 2N5401) [43] is controlled by an NPN transistor (Q3, 2N5551) [44], with the base of Q3 driven by an 8-bit DAC output from the ESP32. Adjusting the DAC voltage allows the microcontroller to modulate the base current of Q2, thereby setting the stimulation current, which is related to the base current via the transistor's current gain.

$$I_{OUT} = I_C(Q2) = I_B(Q2) \times h_{FE}(Q2) \quad (3)$$

Since Q3 directly sources this base current, $I_C(Q3) = I_B(Q2)$, and thus the DAC output controls Iout indirectly via Q3. Applying Ohm's law across R4 gives the collector current of Q3 as:

$$I_C(Q3) = \left(\frac{V_{dac} - V_{BE}(Q3)}{R_4}\right) \quad (4)$$

Combining (3) and (4), the required DAC voltage for a given output current can be expressed as:

$$V_{DAC} = \left(\frac{I_{OUT}}{h_{FE}(Q2)} \times R_4\right) + V_{BE}(Q3) \quad (5)$$

To support a maximum stimulation current of 40 mA with hFE (Q2) = 50, VBE = 0.7 V, and a conservative VDAC (max) = 3.0 V (leaving approximately 10% headroom from the ESP32's 3.3 V theoretical DAC limit), the value of R4 is selected as:

$$R_4 = \left(\frac{(V_{dac} - V_{BE}(Q3)) \times h_{FE}}{I_{OUT}(max)}\right) = \left(\frac{(3.0 - 0.7) \times 50}{0.04}\right) = 2{,}875\Omega \quad (6)$$

A standard value of R_4 = 2.7 kΩ or 3.0 kΩ may be selected depending on design tradeoffs. In this study, R_4 is fixed at 3.0 kΩ, ensuring compatibility with ESP32 DAC output range while maintaining operational margin for BJT gain variation, as implemented in the current-limiting circuit shown in Fig. 4. Using (5-6), the required DAC voltages for output currents of 20-40 mA (in 5 mA increments) are summarized in Table II. All DAC voltages fall within the ESP32's 8-bit DAC output range, validating the design. This indirect current control approach enables safe, energy-efficient, and scalable current delivery, ideal for wearable FES systems requiring compact and flexible stimulation control.

TABLE II
REQUIRED DAC VOLTAGES FOR PROGRAMMABLE OUTPUT CURRENT LEVELS

Level	Iout (mA)	Ib (Q2) (mA)	VDAC (V)
1	20	0.4	1.9
2	25	0.5	2.2
3	30	0.6	2.5
4	35	0.7	2.8
5	40	0.8	3.1

c) Pulse Control Circuit

The pulse control circuit is designed to generate biphasic symmetric stimulation waveforms, which are essential for FES to avoid tissue damage and ensure charge balance across the stimulation electrodes. To accomplish this, the system employs an H-Bridge topology that allows bidirectional current flow between two output terminals [41]. This design enables the generation of alternating positive and negative pulses in response to control signals from the ESP32 microcontroller. As shown in Fig. 5, the H-Bridge consists of four high-voltage transistor pairs: two PNP transistors (Q4 and Q5, 2N5401) [43] at the high side, and four NPN transistors (Q6-Q9, 2N5551) [44] at the low side. The 70 V stimulation voltage is applied at the top of the bridge, and the switching logic from the ESP32 determines which path current will take through the load (electrodes), thus controlling pulse polarity. The base drive for the high-side PNP transistors is provided through resistors R5 and R6, each set to 33 kΩ. These values are chosen to limit the base current to an appropriate level (~1-2 mA) while minimizing unnecessary power dissipation from the high-voltage source. For the low-side NPN transistors, resistors R7-R10 are set to 2.2 kΩ to ensure sufficient base current delivery from the ESP32's 3.3 V digital outputs, enabling fast transistor switching and clean pulse transitions.

This configuration supports stimulation pulses of 100-1000 µs at 10-100 Hz, with resistor values optimized for efficient switching and safe transistor operation. A high-speed diode (D2, BAS516) [45] is placed at the ground rail to suppress reverse transients and protect switching components during polarity changes. This enables precise, safe biphasic stimulation and forms a key link between the power stage and microcontroller logic in a compact design.

2) Sensor Node Design

The sensor node detects heel contact using a Force-Sensing Resistor (FSR) and wirelessly

triggers stimulation. It is built on the M5StickC Plus, an ESP32-based unit with BLE, TFT display, 120 mAh battery, and 4-pin connector for rapid prototyping [46]. Its compact size, onboard battery, and wireless capability make it ideal for wearable use. As shown in Fig. 3 (2), the sensor node consists of a heel pressure sensor and a circuit for signal processing and data transmission.

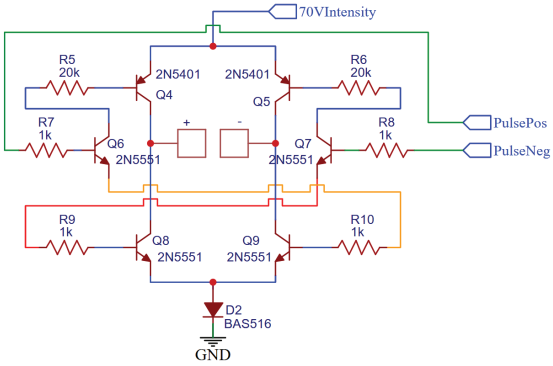

Fig. 5. H-bridge-based pulse control circuit for generating biphasic stimulation waveforms

a) Heel Pressure Sensor Design

To detect heel strike events, a custom force sensor with interdigitated electrodes on a 2-layer PCB detects heel strikes. The 0.8 mm pitch and trace width ensure uniform sensitivity across the 40 × 42 mm sensing area, with enhanced durability under foot pressure. To convert pressure into resistance, a conductive rubber strip (Neo Plastomer Co., Ltd., EP50) with a thickness of 0.6 mm and a nominal resistance range of 20-70 kΩ was placed on top of the electrode array. Under no load, the total resistance between sensor terminals ranged from 800-900 kΩ, and when pressure of approximately 10-15 kgf was applied (as estimated from manual pressing) [47], the resistance dropped to around 500-600 kΩ. This range effectively detects heel contact during walking. A custom sensor was developed due to limited commercial FSR options in the required size and form, with construction designed to endure repeated compression. The layout is shown in Fig. 6.

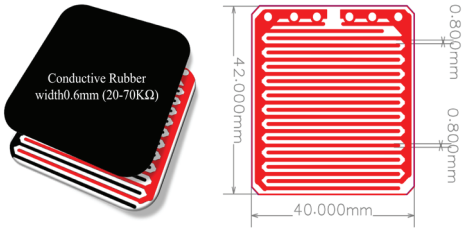

Fig. 6. Custom heel pressure sensor using conductive rubber and interdigitated PCB layout

b) Signal Conditioning and Data Transmission

To interface the sensor with the ESP32's analog-to-digital converter (12-bit ADC), a voltage divider using a 1 MΩ resistor converts the FSR's pressure into a 0.4-2.5 V signal. A 2.0 V threshold was set to detect heel contact, converting the signal to binary for BLE transmission and real-time stimulation control. The interface circuit is shown in Fig. 7.

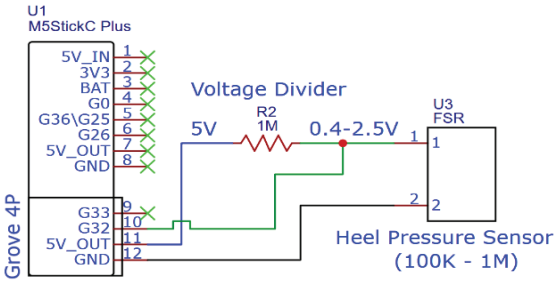

Fig. 7. Voltage divider interface circuit for sensor node using M5StickC Plus

B. *Firmware Design*

The firmware is split between the ESP32-based stimulation and sensor nodes. The stimulation node manages pulse generation, timing, and application communication, while the sensor node handles gait detection, threshold logic, and low-power BLE transmission. Details are provided in the following sections.

1) Firmware for Stimulation Node Design

The stimulation node firmware generates precise biphasic pulses and manages real-time tasks like BLE communication and user control. To achieve microsecond-level accuracy for 100-1000 µs pulses, a 50 µs hardware timer interrupt is used for waveform phase control. The core logic is handled in the pulse control task. Other functions, such as user interface control, BLE reception, cloud logging, and mode selection, run as separate Free RTOS tasks within the loop Task. This task separation ensures responsiveness while avoiding interference with pulse timing, as shown in Fig. 8.

Development used the Arduino Core for ESP32 (v3.1.1) with C/C++. Key libraries include the M5Stack library for hardware control, Free_Fonts library for display, Pub Sub Client library for MQTT, and BLE Device library for BLE server functionality. This implementation enables low-latency, reliable reception of gait triggers for synchronized stimulation. A task-based firmware architecture was adopted to ensure modularity and support future expansion. Two key tasks, pulse Control and signal Logic, handle stimulation timing, intensity, and phase control, ensuring accurate and reliable biphasic waveform generation during operation.

a) Pulse Control Task

The pulse control task handles real-time biphasic stimulation output using a hardware timer interrupt that triggers every 50 µs. The firmware

employs the pulseControl task for pulse control. The Interrupt Service Routine (ISR) is initialized during firmware startup in the setup function, as shown in Fig. 8, where the timer is configured to invoke pulseControl. The task receives timing parameters from the signal Logic task, including pulse duration and waveform phase lengths. During each interrupt, a counter is incremented and compared against these parameters to determine the output state, activating the positive, negative, or idle phase through H-bridge control signals. By isolating time-critical operations in this ISR and delegating logic handling to signal Logic, the system ensures accurate and consistent waveform generation, regardless of background processing load.

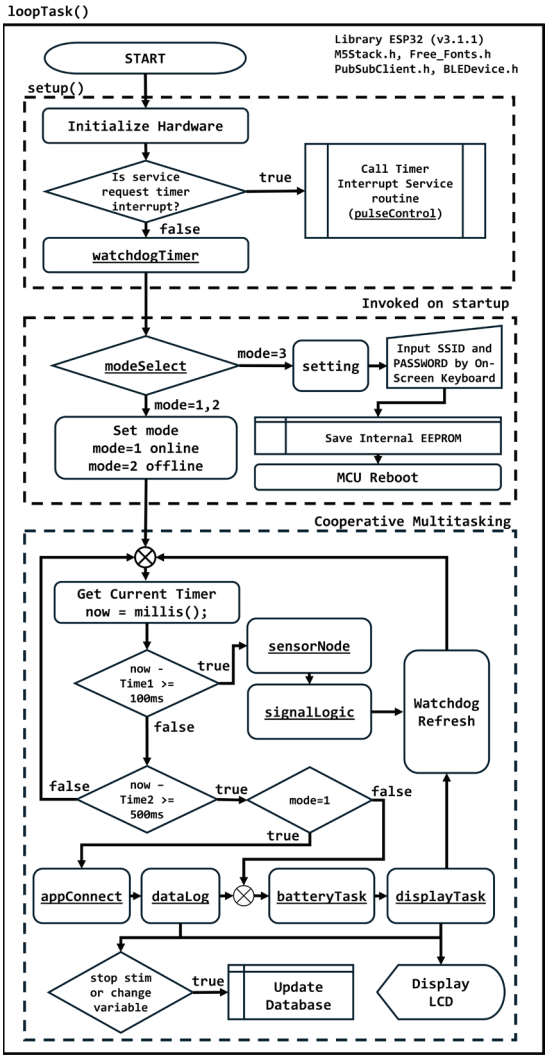

Fig. 8. Firmware execution flowchart of the stimulation node

b) Signal Control Task

The firmware employs the signalLogic task for signal control. This task is responsible for orchestrating the logical control of stimulation behavior, acting as the intermediary between user input, sensor trigger events, and the low-level pulse Control task responsible for waveform output. This task plays a key role in ensuring synchronized, programmable stimulation that adapts dynamically to both manual commands and sensor-based inputs. Within each control cycle, the task evaluates the current stimulation status. This status may originate from two independent sources: a user-defined input, such as pressing a physical button or toggling a mobile application control, or a real-time signal received from the sensor node via BLE, which corresponds to a detected heel strike.

When activated, the signalLogic task sets control flags and prepares waveform parameters. Based on the selected intensity level (1-5), it enables the boost converter via the STDN signal and adjusts the DAC output voltage according to a predefined current map (20-40 mA), regulated by the current limit circuit. For systems using an 8-bit DAC with a 3.3 V reference, the digital value sent to the DAC is calculated by scaling the desired voltage proportionally to the full range of 255 steps. For example, a DAC output of 1.65 V would correspond to roughly half of the maximum digital value.

Another key role of the signalLogic task is to compute timing parameters for each stimulation cycle, including ticks for the positive phase, negative phase, and idle period, based on user-defined pulse duration and frequency. These values, calculated using Equations (7)-(9), are essential for the pulseControl task to generate accurate waveforms.

$$N_{pulse} = \frac{t_{pulse}}{T_{ISR}} \tag{7}$$

$$N_{total} = \frac{1}{f \times T_{ISR}} \tag{8}$$

$$N_{idle} = N_{total} - 2N_{pulse} \tag{9}$$

Equations (7) to (9) define ISR tick counts for each pulse phase and idle period, based on user-defined pulse width and frequency. These values ensure correct waveform structure and are passed to the pulseControl task for real-time output. As shown in Fig. 8, signalLogic operates as a cooperative task at 100 ms intervals and handles key functions such as condition checks, DAC configuration, and tick calculation.

2) Firmware for Sensor Node Design

The sensor node firmware handles periodic heel pressure sensing and low-latency BLE transmission. It uses cooperative multitasking via a loopTask and non-blocking timing with the time function. At each interval, the 12-bit ADC reads sensor voltage, which is compared to a fixed threshold to detect heel strikes, encoded as binary output (1 = detected, 0 = not detected).

The system also monitors battery voltage and estimates its percentage, combining it with the pressure status into a 3-byte data frame. Operating as a BLE GATT server, the sensor node uses a custom

characteristic with notifications to asynchronously transmit data to the stimulation node, which acts as the BLE client.

The firmware was developed using Arduino Core for ESP32 (v3.1.1) in C++, leveraging the M5StickCPlus library for hardware control and the BLEDevice library for wireless communication. This setup enables efficient event detection, low power use, and real-time BLE synchronization with the stimulation node. The execution flow is shown in Fig. 9.

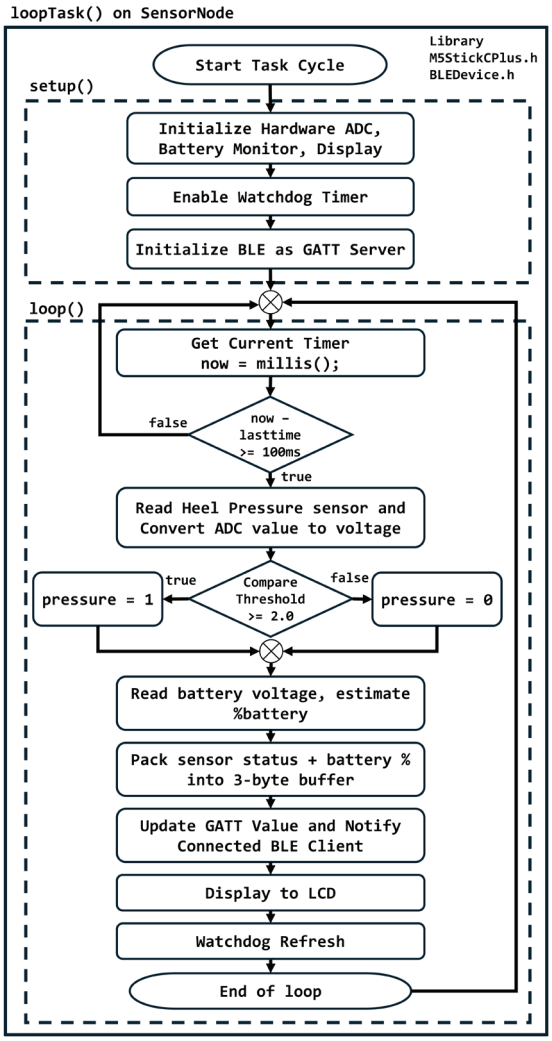

Fig. 9. Flowchart for Sensor Node Design

C. Mobile Health Application (m-Health) Design

The mobile health application (m-Health) developed in this study was designed based on the Technology Acceptance Model for m-Health (MoHTAM) [12] and the design themes proposed by Peng et al. [13], which emphasize perceived ease of use and perceived usefulness.

To improve user control, the application enables adjustment of stimulation parameters, including intensity, frequency, pulse width, and signal smoothness. It also offers pre-configured programs such as muscle relaxation and foot drop routines.

Effective data representation was also a key design objective. As such, the application provides a user-friendly interface that displays personal information, foot drop stimulation history, and the real-time status of stimulation and sensor nodes. The control flow and data representation design are summarized below.

Awareness & Literacy: Onboarding tutorials must be incorporated to familiarize users with the purpose, benefits, and operational procedures of the FES devices prior to engaging with the application.

Time & Effort: The interface is designed to minimize procedural steps and enhance user flow efficiency. Key features include shortcut pathways, One-Time-Password (OTP)-based registration, intuitive navigation structures, and automated stimulation program selection to reduce overall setup time.

Information Needs: Personalized content is delivered through both preset and manual configuration of stimulation parameters. The system also supports multiple-device scenarios for individual users.

Tracking and Feedback: Real-time visual feedback, delivered through charts and status indicators, enables users to effectively monitor stimulation activity and overall device performance.

Reminders: The application must provide users with the option to enable or disable the reminder system, as frequent notifications, whether auditory or visual, may cause annoyance or disrupt the user experience.

D. Communication Design

The system's communication architecture is structured into four layers: 1) the sensor node, which is responsible for collecting physiological data, 2) the stimulation node, which receives data from the sensor node via BLE, acts as the master controller for FES, and transmits data to 3) the cloud server, using the MQTT protocol over a Wi-Fi connection, and 4) the m-Health application, which serves as the user interface layer, supporting interaction and presenting data from the overall system as illustrated in Fig. 10.

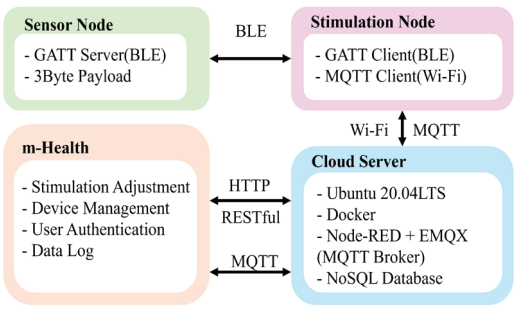

Fig. 10. System communication architecture

The data contained in the BLE payload, communicated between the GATT server and client, was designed to consist of three bytes: 1) the heel pressure state (pressed or unpressed), 2) a separator byte (0x2C), and 3) the battery level represented as a percentage. For example, a data value of 0x01, 0x2C, 0x64 indicates that heel pressure is detected and the battery level is 100%. This structure is optimized for rapid, energy-efficient transmission. The complete data format is described in TABLE III, while its The stimulation node also acts as an MQTT client, communicating with a cloud server hosted on Google Cloud Platform (GCP). The server runs Ubuntu 20.04 LTS with Docker, hosting containers for Node-RED and EMQX (used as an MQTT broker and monitor). Node-RED handles device logic and bridges MQTT messages to NoSQL database services for data logging and user interaction. The mobile health application connects directly to a NoSQL database using HTTP-based RESTful APIs. It provides a frontend interface for displaying system data, controlling stimulation modes, and visualizing user metrics. Communication between the mobile application and cloud backend occurs entirely through a NoSQL database, without requiring direct device-to-app connectivity. This communication design ensures modularity and reliability for distributed control and real-time synchronization.Experimental setup.

TABLE III
THE DESIGNED BLE DATA FORMAT

Byte Index	Description	Data Type	Value Range / Notes
0	Press/Release	uint8_t	0 = not pressed, 1 = pressed
1	Separate	uint8_t	ASCII ‘,’ (0x2C)
2	Battery percent	uint8_t	[0, 100]

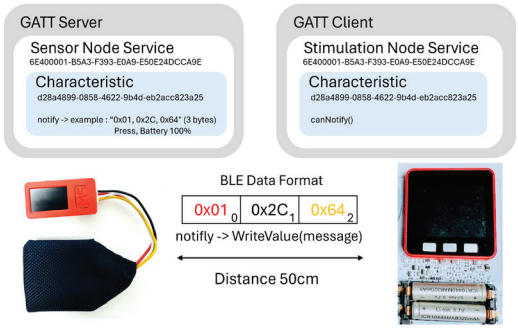

Fig. 11. BLE communication structure between stimulation and sensor nodes with 3-byte payload

To evaluate the performance of the proposed wireless FES system, a series of experimental tests was designed and conducted to assess the accuracy, latency, electrical characteristics, and power efficiency of both the stimulation and sensing modules. The system configuration and test parameters are summarized in TABLE IV. Each test aligns with specific system design domains, including hardware, firmware, communication, and mobile integration, ensuring comprehensive validation across all core components. The five primary experiments were structured as follows, with their respective linkage to system design components.

E. Boost Converter and Current Limit Test

The voltage boosting and current regulation functions of the stimulation node were evaluated in two stages. First, the boost converter (ZXSC410) was tested under open-circuit conditions to confirm voltage elevation from 3.7 V to ~70 V. Second, current regulation was assessed using an RC load (1.75 kΩ 100 nF) across five intensity levels, adjusted via DAC output (1.9–3.1 V). Voltage was monitored with a digital oscilloscope, and current was measured using a multimeter. Results validated the effective operation of both circuits under unloaded and loaded conditions.

F. Timing and Waveform Precision Test

Waveform timing was evaluated by measuring rise/fall times and pulse durations. Using a Rigol DS1022C, the stimulation signal showed sharp transitions under 5 µs and consistent 400 µs biphasic pulses at 50 Hz. Results confirmed accurate timing and waveform stability suitable for nerve stimulation.

G. Sensor Accuracy Test

The Analog-to-Digital Converter (ADC) of the sensor node (ESP32, 12-bit) was validated by comparing its digitized voltage output to a calibrated digital oscilloscope (Siglent SHS810). A heel pressure sensor was used to produce analog voltage values in the range of 0.4-2.5 V via a voltage divider. The sensor node read this voltage via its internal ADC and converted the result back to voltage, which was then compared against reference values from the digital multimeter. A total of 1,000 measurements were collected to compute the mean absolute error and maximum deviation.

TABLE IV
SUMMARY OF SPECIFICATIONS AND TEST PARAMETERS USED IN THE EXPERIMENTAL SETUP

Item	Specification
Stimulation Node Platform	M5Stack (ESP32-based microcontroller)
Sensor Node Platform	M5Stick C Plus (ESP32-based microcontroller)
Sensor	FSR (4x4.2cm pitch 0.8mm) Analog Output
Sampling Rate	10 Hz (100ms)
Wireless Communication Protocol	Bluetooth Low Energy (BLE)
Stimulator Circuit	H-Bridge Driver
Waveform	Symmetric Biphasic
Boost Converter	DC to DC Boost Convertor
Current limit	VDAC with BJT
Stimulation Frequency	50Hz
Stimulation Voltage	±70 V peak-to-peak
Pulse Duration	Positive 400us / Negative 400us
Inter-phase delay	100us
Measurement	Siglent SHS810 and Rigol DS1022C
Stimulation Node Battery	Li-po 3.7v 540mAh (2 × 270 mAh, parallel)
Sensor Node Battery	Li-po 3.7V 120mAh

H. Latency Test

A latency test was conducted to evaluate the communication delay between the sensor node (BLE GATT server) and stimulation node (GATT client) during real-time gait-triggered stimulation. The experiment took place in a 4 × 8 m concrete room with all external communication devices turned off. Both doors and windows were closed to minimize radio interference. The devices were positioned 50 cm apart in a line-of-sight configuration to simulate wearable placement. On the stimulation node, a timestamp was recorded immediately before executing the notifyCallback function. Upon receiving the 3-byte payload from the sensor node, a second timestamp was recorded. The latency (Δt) was calculated as the time difference between these two timestamps. This measurement was repeated 1,000 times, and the data were compiled for statistical analysis.

I. Operation Time and Power Consumption Test

Energy efficiency was evaluated by powering both nodes with internal batteries under continuous operation. New lithium-based cells with fewer than 50 charge cycles were used to minimize degradation effects [48]. The stimulation node, consisting of two parallel 10440 Li-ion cells (3.7 V, 270 mAh each, total 540 mAh), was configured to deliver 70 V biphasic pulses at 40 mA and 50 Hz into a 1.75 kΩ 100 nF load. The sensor node (M5StickC Plus with 3.7 V 120 mAh Li-Po) transmitted heel pressure data via BLE every 100 ms. Battery voltage was sampled every minute using the ESP32's internal ADC, and the system initiated automatic shutdown once voltage dropped below 3.1 V. This threshold was selected based on prior research indicating that operating lithium-ion cells below 3.0 V can accelerate degradation and compromise stability [49]. Continuous runtime was recorded until this cutoff was reached, providing a measure of the system's full-load endurance.

VI. RESULTS

The experimental results are presented in two parts. The first confirms hardware reliability through tests on latency, voltage boosting, current regulation, signal timing, and battery life. The second validates the mobile application's responsiveness, data synchronization, and control over stimulation modes.

A. Hardware System Result

The complete hardware system was successfully fabricated and assembled into a working prototype, comprising a stimulation node and a sensor node with supporting circuits. The final assembled devices are shown in Fig. 12 (a-b). Firmware for both nodes was successfully developed and deployed, Fig. 13 (a-b), enabling pulse generation, BLE communication, battery monitoring, and real-time task execution. In a foot drop use case, the stimulation node was positioned near the common peroneal nerve, and the sensor node under the heel, as illustrated in

Fig. 14 The stimulation device was positioned near the knee to align the electrode with the common peroneal nerve, which lies just below the knee on the lateral side of the leg. Together, Figs. 12-14 highlight the physical realization of the system, from hardware assembly to firmware deployment and electrode placement, demonstrating how the proposed prototype can be applied in a foot drop rehabilitation scenario. To avoid ethical concerns, no human subjects were involved; instead, the study focused on engineering design and functional validation through electrical and communication performance tests. Five key performance categories form the basis for technical evaluation, as outlined in Table V, and detailed in the following sections.

(a) (b)

Fig. 12. Overview of hardware components: (a) stimulation node, (b) sensor node

(a) (b)

Fig. 13. Firmware on hardware (a) firmware on stimulation node (b) firmware on sensor node

Fig. 14. The wireless FES attachment was affixed to the knee and heel.

Performance evaluation of the system was conducted across five core test categories, as summarized in Table V. The circuit was also verified under no-load conditions. A typical output waveform, measured using a Rigol DS1022C oscilloscope at a 400 µs pulse duration with a 100 µs inter-phase interval and 50 Hz frequency, is shown in Fig. 15, confirming that the designed hardware accurately produces symmetrical biphasic waveforms with sharp rise and fall transitions.

The latency test revealed a consistent response time with an average of 6.16 ms and a standard deviation of ±0.88 ms over 1,000 BLE transmission events. The complete latency distribution is presented in Fig. 16, confirming low-latency communication suitable for gait-synchronized stimulation.

TABLE V
SUMMARY OF EXPERIMENTAL RESULTS

Test Item	Description	Result Summary
Latency	Response delay measured from the BLE transmission	1000 samples collected. Average Latency: 6.16 ms SD: ±0.88 ms Max: 8.34 ms Min: 4.91 ms
ADC Module Accuracy	Accuracy of the 12-bit ADC in the sensor node	Vout range: 0.4-2.5 V MAE: 1.2 Max Error: 4 Error < 1.1% Samples: 1000
Boost Converter and Full Load Output Measure-ment	Verification of the voltage boosting capability and output current regulation across programmable intensity levels	Open Circuit Test: - Peak output voltage: 73.6 V - Ripple voltage: ±3.45 V Intensity Test: - L1: 19.35 mA, Err: 3.26% - L2: 25.75 mA, Err: 2.99% - L3: 30.25 mA, Err: 0.85% - L4: 33.42 mA, Err: 4.52% - L5: 39.31 mA, Err: 1.74%
Rise/Fall Time and Pulse Duration	Transition speed and Timing consistency of biphasic 400 µs	Pulse Duration(avg): 400.3 µs Measured rise/fall time: 2.1 µs
Operation Time (Stimula-tion node)	Battery life of the stimulation node under full load	Full system operation at 70 V 40 mA load BLE read every 100 ms Duration: ~4 hours 4m
Operation Time (Sen-sor node)	Battery life of the sensor node during full load	BLE active, convert sensor data every 100 ms Duration: ~1 hour 6m

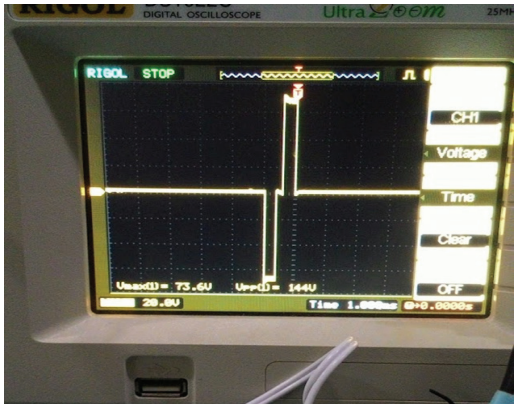

Fig. 15. Symmetrical biphasic waveform measured at 400 µs pulse duration

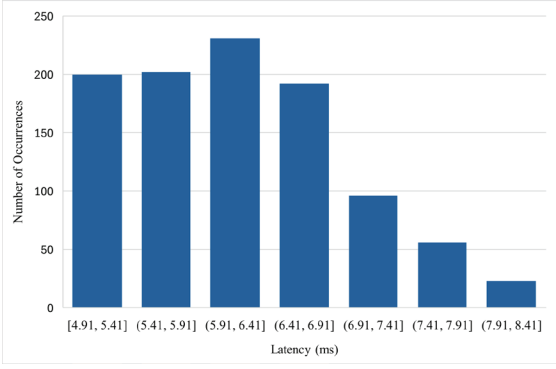

Fig. 16. Distribution of measured BLE latency over 1,000 transmissions

In terms of power management, battery endurance was assessed under continuous full-load conditions over five independent trials. The stimulation node, operating at 70 V and 40 mA, maintained functionality for approximately 4 hours, while the sensor node, transmitting BLE data at 100 ms intervals, operated for over 1 hour. As shown in the voltage discharge curves in Fig. 17, all trials terminated just above 3.1 V, confirming the consistent performance of the power system and proper functioning of the voltage protection mechanism.

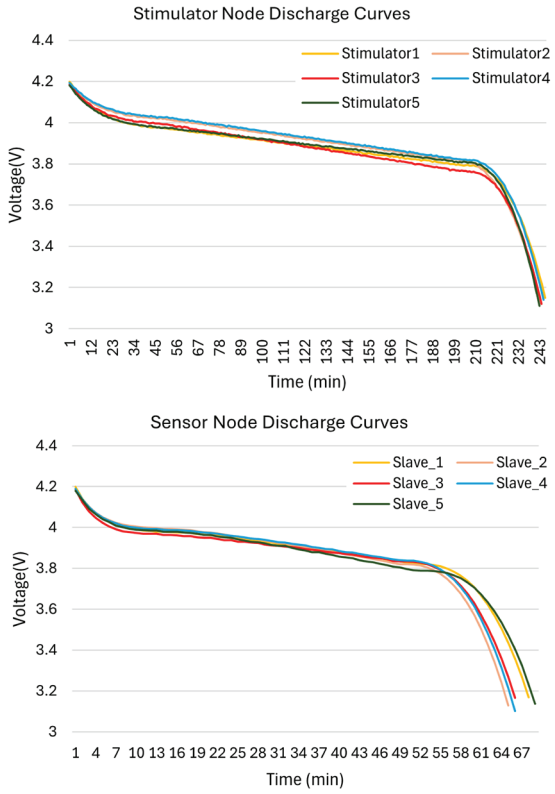

Fig. 17. Battery voltage profile of the stimulation node and sensor node

These results collectively validate the system's functionality, timing precision, power delivery, and wireless communication reliability, supporting its use as a robust, wearable rehabilitation device and a versatile research platform for FES-based neuromuscular interventions.

B. Mobile Health Application Result

The design implications outlined in the previous section were implemented using React Native for the development of the m-Health application in this study. Upon installation, users are directed to a series of welcome screens as illustrated in Fig. 18 (a-c), which introduce the system's objectives and provide guidance on how to use the electrical stimulation features. Users may choose to proceed by tapping the "Continue" button to access more information, or "Skip" to begin using the application immediately. Subsequently, users who have previously registered are automatically signed in. New users are required to register using their email or phone number and a One-Time Password (OTP) sent via SMS, as illustrated in Fig. 19 (a-b).

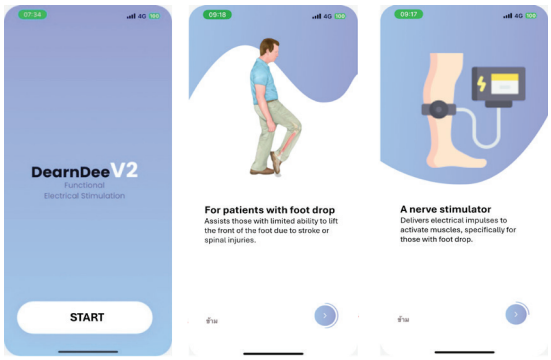

(a) (b) (c)

Fig. 18. (a) Initial welcome screen, (b) example of the system objective screen, and (c) instructional screen for wearing the device

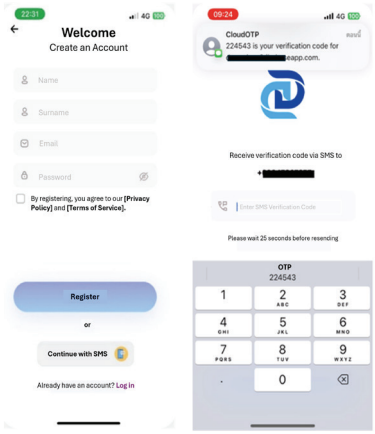

(a) (b)

Fig. 19. (a) Registration screen via email, and (b) registration screen using phone number and One-Time Password (OTP)

Upon entering the application, users are presented with a set of stimulation device management interfaces, as illustrated in Fig. 20 (a) and Fig. 20 (b), which show the device status. These interfaces include screens for adding, deleting, updating, and viewing device information, as well as a usage history screen for monitoring device activity.

After completing the setup tutorial, users are instructed to wear the stimulation node around the knee and place the sensor node near the ankle. They then select the target device from the list shown in Fig. 19 (a). Upon selection, the control interface illustrated in Fig. 21 is displayed, consolidating all available functionalities for operating the stimulation node.

The top section of the interface displays battery levels and communication status for both the stimulation and sensor nodes. Directly below, toggle buttons

allow users to power both devices on and off at the same time. Electrical parameters such as program type, intensity, frequency, signal smoothness, and pulse width can be configured through the interface. In relaxation mode, all parameters except intensity are automatically set based on predefined values stored in the firmware. Users can still manually adjust the intensity level to suit personal comfort and preferences.

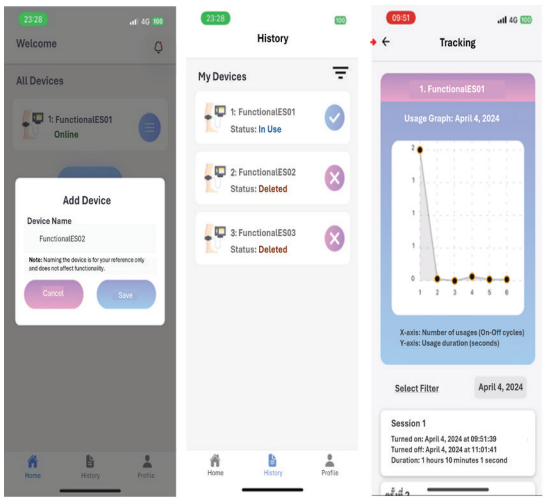

(a) (b) (c)

Fig. 20. (a) Screen for adding stimulation devices, (b) screen for deleting and viewing stimulation devices

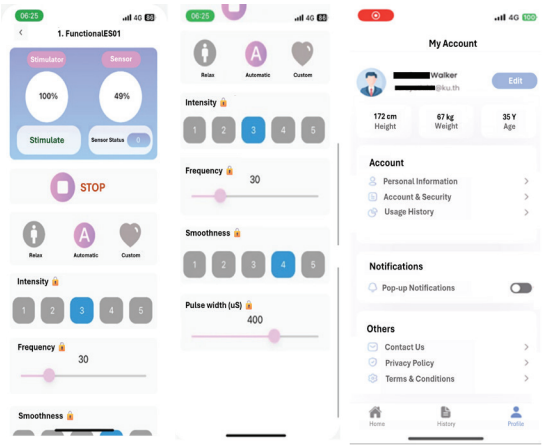

(a) (b) (c)

Fig. 21. (a) Upper section of the stimulation control interface, (b) lower section of the interface

In preset mode, the stimulation node adjusts electrical parameters based on firmware-derived values tailored to the user's physiological profile, activating only upon receiving a sensor signal. In manual mode, user-defined parameters are applied, with activation also triggered by the sensor node.

Lastly, users are provided with a configuration screen that allows them to update their personal information and enable or disable the reminder system through notification messages.

VII. Discussion

This study presents the design and development of a wireless functional electrical stimulation system for foot drop rehabilitation, integrating a stimulation node, a sensor node, a cloud-based data layer, and a mobile health application. The system achieved reliable performance in key areas, including biphasic pulse generation, low-latency BLE communication, real-time parameter control, and mobile feedback.

Experimental validation demonstrated accurate waveform generation (400.3 µs pulse width, 2.1 µs rise/fall time) and stable current delivery across different loads. BLE latency averaged 6.16 ms, meeting the <50 ms threshold for real-time gait stimulation [50]. Power tests showed the stimulation node operated for ~4 hours, while the sensor node lasted ~1 hour.

The wireless architecture posed engineering challenges, addressed by using interrupt-driven firmware for microsecond-level control and cooperative multitasking for reliable BLE communication and UI handling within ESP32 constraints.

The functionality and workflow of the mobile application developed in this study cover rehabilitation activities, providing a module for parameter adjustment and real-time feedback from the installed sensors.

Despite its strengths, the system has limitations. Clinical effectiveness is unverified due to the absence of human testing. The use of a single heel pressure sensor may not fully capture complex gait patterns, and the sensor node's limited battery life and lack of closed-loop current control restrict long-term use and precise stimulation.

Compared to prior FES systems, this design offers advantages in modularity, portability, and integration. While previous works often lacked mobile interfaces or relied on fixed setups, the proposed system combines open-source hardware, real-time BLE, and mobile-cloud support, making it well-suited for home-based rehabilitation. In contrast to a previously deployed wired FES system [11], the present design enhances portability, user control, and home-based applicability through wireless communication and mobile application integration. In comparison with commercial devices such as the Bioness L300 Go [31] or WalkAide [32], which offer advanced features but at high cost, the proposed system provides a more accessible solution. Similarly, compared with recent academic prototypes, which often sacrifice mobile integration or connectivity to maintain low cost, this work achieves a balanced approach that bridges the gap between expensive commercial systems and limited academic designs.

VIII. Conclusion and Future Work

This work demonstrates the feasibility of a low-cost, wireless FES system that integrates real-time stimulation control, BLE-based sensor input, and mobile-cloud connectivity. The system performed reliably across electrical, communication, and software layers, supporting its potential use for home-based rehabilitation in foot drop patients.

Future development will focus on enhancing sensor flexibility by integrating IMU or sensor-less gait analysis, improving battery life through optimized power management, and implementing closed-loop current control to ensure stimulation accuracy. Clinical testing with human participants is also essential to evaluate usability, therapeutic outcomes, and long-term effectiveness.

Funding: This research received no external funding.

Data Availability Statement: The original contributions presented in the study are included in the article; further inquiries can be directed to the corresponding author on reasonable request.

Acknowledgments: The authors would like to thank the Faculty of Engineering at Sriracha, Kasetsart University, for providing the facilities for experimentation.

Conflicts of Interest: The authors declare no conflicts of interest.

References

[1] V. L. Feigin et al., "World Stroke Organization (WSO): Global stroke fact sheet 2022," *Int. J. Stroke*, vol. 17, no. 1, pp. 18-29, Jan. 2022, https://doi.org/10.1177/17474930211065917

[2] S. L. Nori and M. F. Stretanski, *Foot Drop.* Treasure Island, FL, USA: StatPearls Publ., 2025.

[3] D. Totah, M. Menon, C. Jones-Hershinow, K. Barton, and D. H. Gates, "The impact of ankle-foot orthosis stiffness on gait: A systematic literature review," *Gait Posture*, vol. 69, pp. 101-111, Jan. 2019.

[4] P. Chayaratanasin, S. Vongpipatana, and W. Chira-Adisai, "Comparison of gait pattern during walking with and without functional electrical stimulation 'Dearndee™' in stroke patients with foot drop: A pilot study," *ASEAN J. Rehabil. Med*., vol. 25, no. 2, pp. 65-72, Aug. 2015.

[5] S. Kumnoonsup, M. Buntragulpoontawee, and A. Kovindha, "Effectiveness of functional electrical stimulator (FES-Dearndee™) on physiological cost index in subacute stroke patients with foot drop: A pilot study," *ASEAN J. Rehabil. Med.*, vol. 25, no. 3, pp. 95-102, Dec. 2015.

[6] A. Behboodi, N. Zahradka, H. Wright, J. Alesi, and S. C. Lee, "Real-time detection of seven phases of gait in children with cerebral palsy using two gyroscopes," *Sensors*, vol. 19, no. 11, p. 2517, Jun. 2019.

[7] Y. R. Mao et al., "Spatiotemporal, kinematic and kinetic assessment of the effects of a foot drop stimulator for home-based rehabilitation of patients with chronic stroke: A randomized clinical trial," *J. Neuroeng. Rehabil.*, vol. 19, no. 1, p. 56, Dec. 2022, https://doi.org/10.1186/s12984-022-01036-0/

[8] D. B. Popović, "Foot drop stimulator," in *Handbook of Biochips*, M. Sawan, Ed. New York, NY, USA: Springer, 2022, pp. 1241-1255.

[9] F. Alnajjar, R. Zaier, S. Khalid, and M. Gochoo, "Trends and technologies in rehabilitation of foot drop: A systematic review," *Expert Rev. Med. Devices*, vol. 18, no. 1, pp. 31-46, Jan. 2021, https://doi.org/10.1080/17434440.2021.1857729

[10] A. E. Carolus, M. Becker, J. Cuny, R. Smektala, K. Schmieder, and C. Brenke, "The interdisciplinary management of foot drop," *Dtsch. Arztebl. Int.*, vol. 116, no. 20, pp. 347-354, 2019.

[11] J. Jitprasutwit, R. Chaiwattanatham, and Z. Lertmanorat, "Development and distribution of functional electrical stimulator for foot drop for Thais," in *Proc. 8th Biomed. Eng. Int. Conf. (BMEiCON*), 2015, pp. 1-4.

[12] A. H. H. Mohamed, H. Tawfik, D. Al-Jumeily, and L. Norton, "MoHTAM: A technology acceptance model for mobile health applications," in *Proc. Developments E-Syst. Eng.*, 2011, pp. 13-18.

[13] W. Peng, S. Kanthawala, S. Yuan, and S. A. Hussain, "A qualitative study of user perceptions of mobile health apps," *BMC Public Health*, vol. 16, no. 1, p. 1158, Dec. 2016, https://doi.org/10.1186/s12889-016-3808-0

[14] A. Kralj and T. Bajd, *Functional Electrical Stimulation: Standing and Walking after Spinal Cord Injury*. Abingdon, U.K: Routledge, 2022, p. 208.

[15] J. S. Park, S. H. Lee, W. G. Yoo, and M. Y. Chang, "Immediate effect of a wearable foot drop stimulator to prevent foot drop on the gait ability of patients with hemiplegia after stroke," *Assist. Technol.*, vol. 33, no. 6, pp. 313-317, Nov. 2021, https://doi.org/10.1080/10400435.2019.1634658

[16] G. Hsu, F. Farahani, and L. C. Parra, "Cutaneous sensation of electrical stimulation waveforms," *Brain Stimul.*, vol. 14, no. 3, pp. 693-702, 2021.

[17] C. Marquez-Chin and M. R. Popovic, "Functional electrical stimulation therapy for restoration of motor function after spinal cord injury and stroke: A review," *Biomed. Eng. Online*, vol. 19, no. 1, p. 34, Dec. 2020, https://doi.org/10.1186/s12938-020-00773-4

[18] A. S. Gorgey, H. J. Poarch, D. D. Dolbow, T. Castillo, and D. R. Gater, "Effect of adjusting pulse durations of functional electrical stimulation cycling on energy expenditure and fatigue after spinal cord injury," *J. Rehabil. Res. Dev.*, vol. 51, no. 9, pp. 1455-1468, Aug. 2014.

[19] Espressif Systems, "ESP32 Bluetooth Architecture," *Espressif*, 2025. [Online]. Available: https://www.espressif.com/sites/default/files/documentation/esp32_bluetooth_architecture_en.pdf. [Accessed: May 19, 2025].

[20] D. Hercog, T. Lerher, M. Truntič, and O. Težak, "Design and implementation of ESP32-based IoT devices," *Sensors*, vol. 23, no. 15, p. 6739, Jul. 2023.

[21] S. D. Bhattacharya and M. Manjunatha, "Functional electrical stimulation on improving foot drop gait in poststroke rehabilitation: A review of its technology and clinical efficacy," *Crit. Rev. Biomed. Eng.*, vol. 41, no. 2, Jan. 2013.

[22] P. L. Melo, M. T. Silva, J. M. Martins, and D. J. Newman, "Technical developments of functional electrical stimulation to correct drop foot: sensing, actuation and control strategies," *Clin Biomech*, vol. 30, no. 2, pp. 101-113, 2015.

[23] T. Watanabe, S. Endo, and R. Morita, "Development of a prototype of portable FES rehabilitation system for relearning of gait for hemiplegic subjects," *Healthc. Technol. Lett.*, vol. 3, no. 4, pp. 284-289, Dec. 2016, https://doi.org/10.1049/htl.2016.0045

[24] P. Aqueveque et al., "A novel capacitive step sensor to trigger stimulation on functional electrical stimulators devices for drop foot," *IEEE Trans. Neural Syst. Rehabil. Eng.*, vol. 28, no. 12, pp. 3083-3088, Jan. 2020.

[25] G. York and S. Chakrabarty, "A survey on foot drop and functional electrical stimulation," *Int. J. Intell. Robot. Appl.*, vol. 3, no. 1, pp. 4-10, Mar. 2019, https://doi.org/10.1007/s41315-019-00088-1

[26] K. Kipli, M. N. Ulia, L. Roslan, A. Jamali, and N. Soin, "Functional Electrical Stimulation (FES) study for foot drop rehabilitation using Arduino Nano Atmega328p," in *Proc. 4th Int. Conf. Innov. Biomed. Eng. Life Sci. (IFMBE P)*, vol. 107, 2024, pp. 242-249, https://doi.org/10.1007/978-3-031-56438-3_24
[27] T. F. De Almeida, L. H. B. Borges, and A. F. O. de A. Dantas, "Development of an IoT electrostimulator with closed-loop control," *Sensors*, vol. 22, no. 9, p. 3551, 2022.
[28] N. Gangadharan, S. Balasubramanian, G. Tharion, J. John, T. Senthilvelkumar, and S. Devasahayam, "An intelligent system for automatic footdrop correction in stroke patients using FES: A pilot study," *Int. J. Sci. Eng. Res.*, vol. 10, no. 4, pp. 1102-1110, Apr. 2019.
[29] O. A. Chiriac, F. C. Adochiei, N.-I. Trocan, and M. I. Nistor, "Design and implementation of a cost-effective, functional electrical stimulation device for foot drop rehabilitation," *Rev. Roum. Sci. Tech. Electrotech. Energ.*, vol. 70, no. 1, pp. 151-156, 2025.
[30] Y. Cao et al., "Development of a wearable ultrasound–FES integrated rehabilitation and motor-functional reconstruction system for post-stroke patients," *Biomed. Signal Process. Control*, vol. 100, p. 106846, Feb. 2025.
[31] Bioness, "L300 Go System for foot drop," *BionessMedical*, 2025. [Online]. Available: https://bionessmedical.com/l300/ [Accessed: Jan. 19, 2025].
[32] BioMetrics Prosthetic and Orthotic CT, "WalkAide® System for foot drop," *BioMetrics*, 2025. [Online]. Available: https://biometricsct.com/custom-orthopedic-care/walkaide/ [Accessed: May 19, 2025].
[33] XFT, "Foot Drop System (XFT-2001D)," *China*, 2025. [Online]. Available: https://www.xft-china.com/foot-drop-system [Accessed: Jan. 19, 2025].
[34] X. I. E. Chunhu and C. Liu, "Functional electrical stimulation therapeutic apparatus for foot drop," China, CN Patent 113965021 B, Aug. 9, 2022.
[35] T. Keller, N. Malesevic, and G. Bijelic, "System and method for functional electrical stimulation," U.S. Patent 10,772,544, Sep. 15, 2020.
[36] M. T. Anton, H. M. Greenberger, E. Andreopoulos, and R. L. Pande, "Evaluation of a commercial mobile health app for depression and anxiety (Able to Digital+): Retrospective cohort study," *JMIR Form. Res*., vol. 5, no. 9, p. e27570, Sep. 2021.
[37] S. Rianmora and S. Seng, "Keep It Cool' smart bag by Internet of Things (IoT) for better living with alternative design," *Int. Sci. J. Eng. Technol. (ISJET)*, vol. 5, no. 2, pp. 38-54, Dec. 2021.
[38] K. Wongwut, C. Chaisermvong, and D. Angamnuaysiri, "The development of smart farming system for sea lettuce cultured process," *Int. Sci. J. Eng. Technol. (ISJET)*, vol. 8, no. 2, pp. 47-53, Dec. 2024.
[39] M5Stack, "M5Stack Basic Development Kit,' M5Stack documentation." *M5Stack*, 2025. [Online]. Available: https://docs.m5stack.com/en/core/basic [Accessed: May 19, 2025].
[40] ON Semiconductor, "2N5401: PNP silicon transistor, datasheet, Rev. 2.1," *Onsemi*, 2025. [Online]. Available: https://www.onsemi.com/pdf/datasheet/2n5401-d.pdf [Accessed: Feb. 19, 2025].
[41] H. Nisar, A. R. Malik, M. Asawal, and H. M. Cheema, "An electrical stimulation based therapeutic wearable for pressure ulcer prevention," in *Proc. IEEE EMBS Conf. Biomed. Eng. Sci. (IECBES)*, 2016, pp. 411-414.
[42] Diodes Inc., "ZXSC410: Voltage mode boost controller." *Diodes*, 2025. [Online]. Available: https://www.diodes.com/part/view/ZXSC410 [Accessed: Feb. 19, 2025].
[43] ON Semiconductor, "2N5401: PNP silicon transistor, datasheet, Rev. 2.1," *On Semiconductor*, 2025. [Online]. Available: https://www.onsemi.com/pdf/datasheet/2n5401-d.pdf [Accessed: Feb. 19, 2025].
[44] ON Semiconductor, "2N5551: NPN silicon transistor, datasheet, Rev. 6," *On Semiconductor*, 2025. [Online]. Available: https://www.onsemi.com/download/data-sheet/pdf/2n5551t-d.pdf [Accessed: May 19, 2025].
[45] Nexperia, "BAS516: High-speed switching diode, datasheet," *Nexperia*, 2025. [Online]. Available: https://www.nexperia.com/product/BAS516 [Accessed: May 19, 2025].
[46] M5Stack, "M5StickC Plus Development Kit,' M5Stack documentation," *M5Stack*, 2025. [Online]. Available: https://docs.m5stack.com/en/core/m5stickc_plus [Accessed: May 19, 2025].
[47] S. Aali, F. Rezazadeh, G. Badicu, and W. R. Grosz, "Effect of heel-first strike gait on knee and ankle mechanics," *Medicina*, vol. 57, no. 7, p. 657, Jun. 2021.
[48] P. Keil and A. Jossen, "Charging protocols for lithium-ion batteries and their impact on cycle life—an experimental study with different 18650 high-power cells," *J. Energy Storage*, vol. 6, pp. 125-141, May. 2016.
[49] G. J. Páez Fajardo et al., "Synergistic degradation mechanism in single crystal Ni-rich NMC//graphite cells," *ACS Energy Lett*., vol. 8, no. 12, pp. 5025-5031, Dec. 2023, https://doi.org/10.1021/acsenergylett.3c01596

Jirawat Jitprasutwit is a lecturer in the Department of Computer Engineering, Faculty of Engineering at Sriracha, Kasetsart University Sriracha Campus,Thailand. He received an M. Eng. in Electrical Engineering from Mahidol UniversityThailand. His research , interests include biomedical engineering, Artificial Intelligence, Internet of Things, embedded systems, and smart intelligent systems.

Anan Banharnsakun is an Associate Professor in the department of computer engineering, Faculty of Engineering at Sriracha, Kasetsart University, Campus, Thailand. He received a Ph.D. degree in Electrical and Computer engineering from King Mongkut's University of Technology Thonburi (KMUTT), Thailand. His research interests include biologically inspired computational intelligence, robust optimization, pattern recognition, and high-performance computing.

Kathawach Satianpakiranakorn is a lecturer in the Department of Computer Engineering, Faculty of Engineering at Sriracha, Kasetsart University, Sriracha Campus, Thailand. He received M.Eng. in Computer Applied Technology from Harbin Engineering University, P.R. Harbin, China. His research field includes Artificial Intelligence, computer vision, and digital image processing.

Kanjana Eiamsaard is an Assistant Professor in the department of computer engineering, Faculty of Engineering at Sriracha, Kasetsart University Sriracha Campus, Thailand. She received an M.S. in Software Engineering from Chulalongkorn University, Thailand. Her research interests include Artificial Intelligence, machine learning, and software engineering.